International Journal of Research In Vocational Studies (IJRVOCAS)
Vol. 4, No. 2 August 2024, pp. 01~09
Print ISSN 2777-0168| Online ISSN 2777-0141| DOI prefix: 10.53893
https://journal.gpp.or.id/index.php/ijrvocas/index

Combine Improvement for Dye-Sensitized Solar Cells: Characterization of Metal Oxide-Doped TiO_2 Nanoparticles Integrated with *Clitoria Ternatea* Extract

Ronaldo, Rusdianasari* & Abu Hasan

Department of Renewable Energy Engineering, Politeknik Negeri Sriwijaya, Jl. Srijaya Negara Bukit Besar, Palembang, 20139, Indonesia

Email address:

rusdianasari@polsri.ac.id

*Corresponding author

To cite this article:

Ronaldo, Rusdianasari, & Hasan, A. Combine Improvement for Dye-Sensitized Solar Cells: Characterization of Metal Oxide-Doped TiO2 Nanoparticles Integrated with Clitoria Ternatea Extract. International Journal of Research in Vocational Studies (IJRVOCAS), 4(2). https://doi.org/10.53893/ijrvocas.v4i2.292

Received: 07 12, 2024; **Accepted**: 08 20, 2024; **Published**: 08 31, 2024

Abstract: Dye Sensitized-Solar Cells (DSSC) represent a third-generation solar cell technology based on photoelectrochemical principles. This study explores the use of *Clitoria ternatea* (butterfly pea) extract as an organic dye for DSSCs, focusing on its ability to absorb sunlight effectively. Excitation of electrons triggered by light in photocatalysis is strongly influenced by the position of the band gap. To be effective as a photocatalyst, the material must have a conduction band with a high positive potential compared to the electron accepting potential. Doping metal oxides such as CuO, MgO, Fe_2O_3, and ZnO into TiO_2 can change the band edge properties or surface states which can increase light absorption. This research presents the synthesis of TiO_2 nanoparticles as photoanodes doped using metal oxides to evaluate characteristic that can influence DSSC performance. TiO_2 nanoparticles doped with metal oxide were synthesized using the solvothermal method and characterized by XRD, SEM-EDX, FTIR, and UV-Vis. Comprehensive analysis of samples doped with metal oxides significantly affects the crystal structure, morphology, elemental composition, and optical properties of the material. The results showed that Cu-doped TiO_2 samples allowed for the most significant performance improvement in DSSC, followed by Fe-doped TiO_2, Mg-doped TiO_2, and Zn-doped TiO_2, with pure TiO_2 having the lowest performance potential. These results provide important insights into material optimization to improve DSSC efficiency.

Keywords: DSSC, Photoanode, Metal Oxide, *Clitoria Ternatea*

1. Introduction

One solution for the energy requirements of the future is renewable energy. Even if this system just uses solar energy and offers an endless supply of clean energy, there are several real-world issues that need to be considered[1]. Electricity generation through light energy, particularly using Dye-Sensitized Solar Cells (DSSC), has garnered significant research interest due to its potential for cost-effective and sustainable energy production. Apart from conventional solar cell technology, third-generation solar cell technology such as DSSC shows potential as a more economical solution[2], [3], [4], [5]. The ratio of the energy output from solar cells to the energy inputs that are absorbed from the sun is known as efficiency. A DSSC's efficiency can used as a gauge to turn solar energy into electrical energy[6]. Photon conversion efficiency in flexible solar cells is still relatively low, around 2-3%, the main problem is high recombination reactions due to poor connections between nanoparticles on the photoanode surface. Efforts continue to be made to increase efficiency and reach its full potential as a flexible and efficient energy source[4], [7].

In DSSC, the conductive glass substrate is coated with a mesoporous nanocrystalline material that has a wide bad gap.

A layer of dye molecules is used as a photoanode which is sensitive to light. An electrolyte in the form of an organic solvent containing the iodide/triiodide redox pair is used to transfer electrons between the photoanode and the counter electrode. Counter electrodes are usually made of platinum or carbon-based materials which are effective as triiodide reduction catalysts. With this mechanism, dye solar cells can convert light energy into electrical energy[2]. DSSC has the advantage of absorbing light from various wavelengths, including in low light conditions, as well as the ability to work in indirect light[5].

Titanium dioxide (TiO_2) has many interesting applications in a variety of fields, including as a highly desirable photoanode material in DSSCs[5], [8]. To increase the photocatalytic activity of TiO_2, the addition of metal ions to TiO_2 has been proven to be effective. This is caused by a decrease in the band gap energy and a shift of the TiO_2 absorption edge to the visible region. The presence of metal ions can also increase the electron capture rate and reduce electron-hole recombination, which in turn increases the efficiency of TiO_2 photocatalysis[9].

TiO_2 can only absorb UV light, this is because there is a large energy band gap which affects the efficiency of TiO_2 based solar cells[10]. The use of metal particles in a photovoltaic system can increase the efficiency and performance of the device[11]. Doping metals such as Cu, Fe, Mg, and Zn on TiO_2 can effectively separate electron-hole pairs induced by light so that optimal balance is achieved[4], [9], [12], [13], [14], [15].

Another effort that can also increase DSSC efficiency is selecting dyes as sensitizers. The use of natural dyes in DSSC has several advantages, including sustainability and environmental friendliness[16]. Dyes in DSSC, when exposed to sunlight, the electronic structure of the pigment changes, causing a change in wavelength and allowing the conversion of light energy into electrical energy[17].

The *Clitoria ternatea* flower is an alternative in selecting a photosensitizer. This is because it contains anthocyanin color pigments which have a high level of light transmission. Solvents such as methanol, ethanol, acetone, water, and water mixtures are used in anthocyanin extraction[18].

DSSC is a semiconductor device that operates based on the conversion of solar radiation into electrical energy[19]. DSSC efficiency has increased from about 7% to about 14%[20]. The DSSC device consists of several main components that form a sandwich structure[21]. Photoanode plays a very important role in DSSC. To achieve high light absorption efficiency, the nanostructured metal oxide semiconductor layer must have high roughness, which results in a large surface area, which in turn increases the chance of electron transfer from the sensitizer to the semiconductor layer[22].

The semiconductor material used in photoanode, such as TiO_2, plays a role in absorbing sunlight and producing stimulated electrons. Apart from that, the photoanode also acts as a transportation medium to transport these electrons to the counter electrode via the electrolyte[17].

2. Material and Method

2.1. Material

The materials used are Butterfly Pea Flowers, Titanium Dioxide (TiO_2 98%), Magnesium Oxide (MgO 99%), Zinc Oxide (ZnO 99%), Iron III Oxide (Fe_2O_3 99%), Copper II Oxide (CuO 99%), Ethanol (C_2H_6O 96%), and Hydrochloric Acid (HCl 37%) are used as commercial chemicals of ROFA.

2.2. Synthesis of Photoanode Nanoparticles

Synthesis of photoanode nanoparticles was carried out using the solvothermal method. 50 grams of TiO_2 was dissolved in 500 mL of ethanol solvent in a ratio of 1:10 using a beaker. Then the metal oxides MgO, Fe_2O_3, CuO, and ZnO in amounts of 0.5 grams each were dissolved in HCl solution with a doping percentage of 5% of the amount of TiO_2 used. Next, TiO_2 which has been dissolved in ethanol is then mixed with metal oxides which have been dissolved in HCl in a chemical beaker. Then the mixture was stirred using a magnetic stirrer on a hotplate at a temperature of 90 ºC for 3 hours until the solution thickened. Next, TiO_2 which has been doped with each metal oxide is put into a desiccator and left for 12 hours to reduce the water content still contained in the mixture. Once complete, the mixture was calcined using a furnace at a temperature of 450 ºC for 3 hours using a porcelain cup to form metal doped TiO_2 crystals. Then the metal doped TiO_2 crystals were crushed using a mortar until smooth and then stored in dark vials and labeled with each sample.

2.3. Dye Extraction

Clitoria ternatea is extracted using the maceration method. Dried *Clitoria ternatea* cut into small sizes. The prepared *Clitoria ternatea* was then added with ethanol solvent in a ratio of 1:6 (w/v) which had been acidified with 3 mL (0.2%) of HCl. Next, the sample was stored in a bottle for 24 hours at room temperature in the dark. After the extraction process is complete, the filtrate is filtered using filter paper to separate the butterfly pea flower residue. The dye extract obtained is then stored in a vial that has been coated with aluminum foil to be used as a photosensitizer.

2.4. DSSC Characterization

The characterization carried out at DSSC is structural characterization using X-Ray Diffraction (XRD) to analyze the crystal structure of the material. Morphology and composition characterization uses Scanning Electron Microscope-Energy Dispersive X-Ray (SEM-EDX) to examine the surface morphology and composition of the sample. Chemical characterization uses Fourier Transform Infrared Spectroscopy (FTIR) to identify functional groups in the molecules of a compound. Optical characterization was carried out using a UV-Vis Spectrophotometer to characterize the light absorption spectra of the dye.

3. Result and Discussion

3.1. Structural Characterization

X-Ray Diffraction (XRD) analysis is a structural characterization technique that is used to determine and analyze the presence and crystal phase of the photoanode material. A Rigaku Miniflex 300/600 instrument was used to create the XRD graphs. It was set to scan between 5-90 deg per minute with a step size of 0.02 deg. Figure 1 displays the result of the diffractogram. Representative samples of Fe-doped TiO_2, Zn-doped TiO_2, Mg-doped TiO_2, and Cu-doped TiO_2 are shown in Figures 1(a), 1(b), 1(c), and 1(d), in that order.

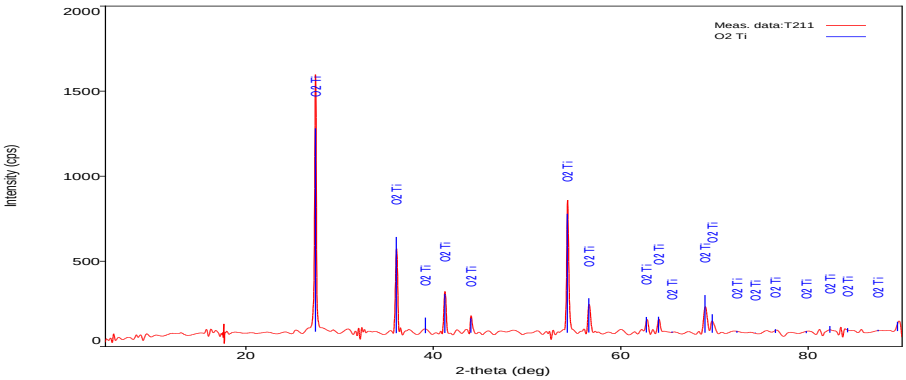

(a)

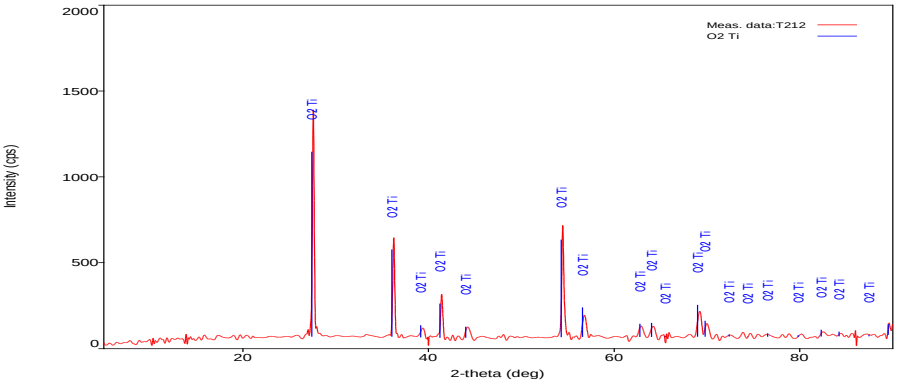

(b)

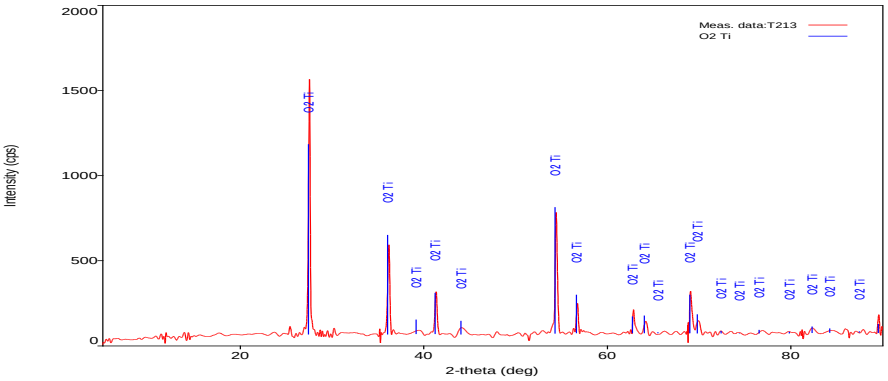

(c)

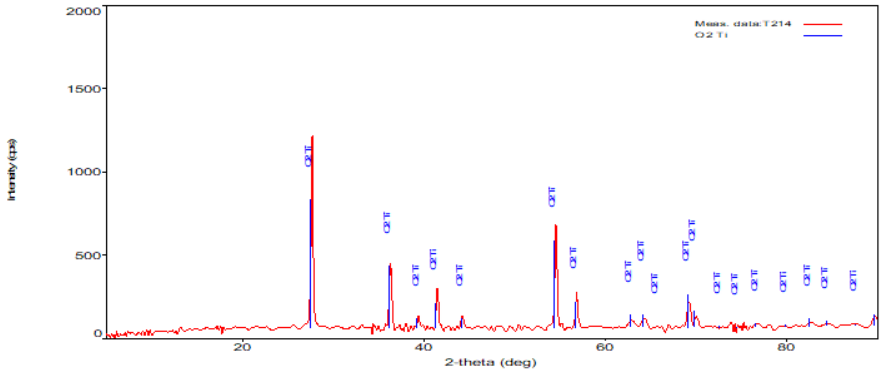

(c)

Figure 1. *Results of XRD Analysis Difratogram: (a) Fe-doped TiO_2, (b) Zn-doped TiO_2, (c) Mg-doped TiO_2, dan (d) Cu-doped TiO_2*

The results of XRD analysis use the Williamson-Hall method and can be seen in Table 1.

Table 1. *Results of XRD analysis on samples doped with metal oxide nanoparticles on TiO_2*

Sample	Crystal Size (Å)	Strain (%)	Space Group	Phase	Crystal Form
Fe-doped TiO_2	359.5(12)	0.15(3)	136 : P42/mnm	Anatase	Tetragonal
Zn-doped TiO_2	397.58(12)	0.076(4)	136 : P42/mnm	Anatase	Tetragonal
Mg-doped TiO_2	295.0(13)	0.20(4)	136 : P42/mnm	Anatase	Tetragonal
Cu-doped TiO_2	256.4(6)	0.15(3)	136 : P42/mnm	Anatase	Tetragonal

XRD analysis confirmed that all samples are in the TiO2 anatase phase, which is known for its high photoactivity, making it ideal for DSSC application. The crystal size of the Zn-doped TiO_2 sample had the largest crystal size of 397.58 Å. A larger crystal size means less grain boundary, which can reduce the rate of charge-carrier recombination produced by light.

Meanwhile, the Mg-doped TiO_2 sample has the smallest crystal size, which is 293.01Å. Smaller crystal sizes can increase the surface area which is beneficial for dye adsorption but can also increase charge recombination due to more grain boundaries.

Judging from the strain factor, the Mg-doped TiO_2 sample showed the highest strain of 0.20%, which showed significant lattice distortion. High strain can introduce a defect state that has the potential to enhance charge separation but can also act as a recombination center.

Zn-doped TiO_2 is expected to provide the best performance for DSSC due to its large crystal size and low strain resulting in efficient electron transport and low recombination rates. Fe-doped TiO_2 and Cu-doped TiO_2 followed due to the smaller crystal size. Mg-doped TiO_2 is expected to provide moderate performance due to the trade-off between high surface area and increased recombination rate due to smaller crystal size and higher strain.

3.2. Morphological and Compositional Characterization

Morphological characterization using Scanning Electron Microscopy (SEM) analysis provides a visual picture of morphology and structural changes due to doping, while composition characterization using Dispersive X-Ray Spectroscopy (EDX) analysis provides confirmation of elemental composition showing the successful doping of each metal into the TiO_2 matrix. The results of the SEM-EDX analysis can be seen in Figure 2 and Table 2.

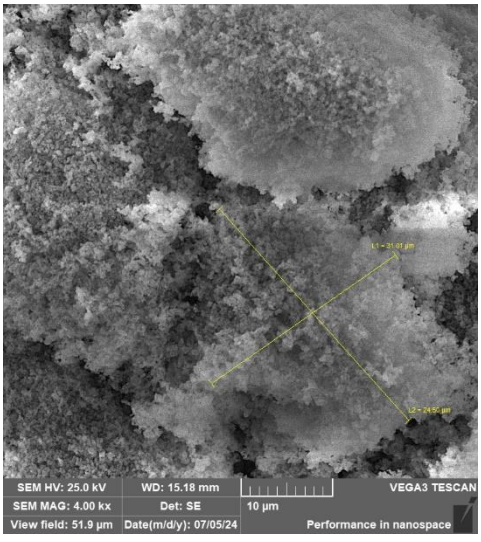

(a)

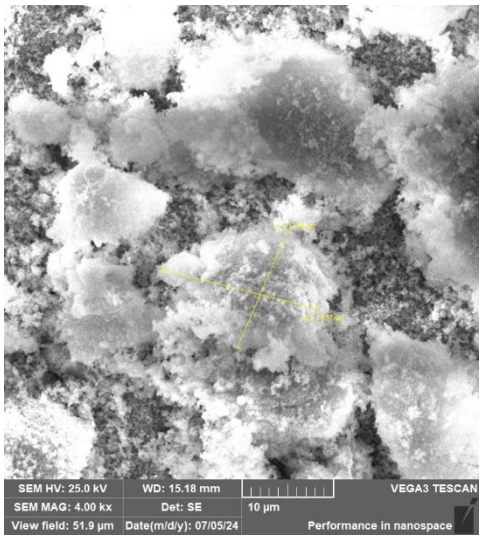

(b)

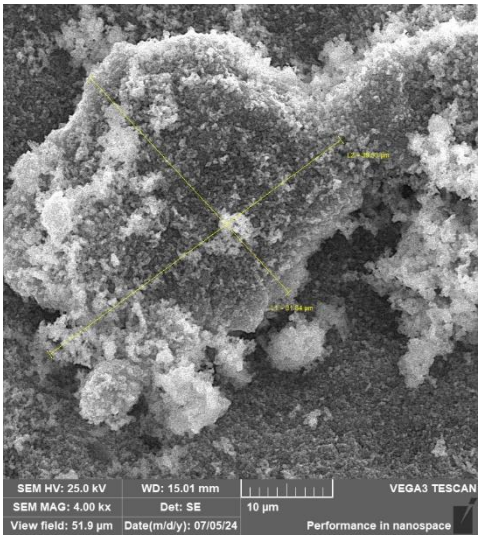

(c)

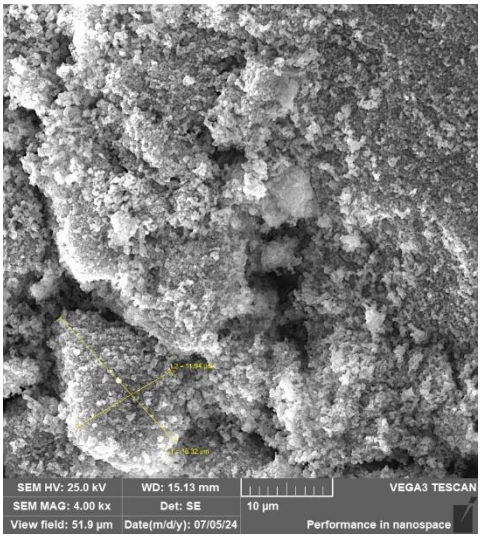

(d)

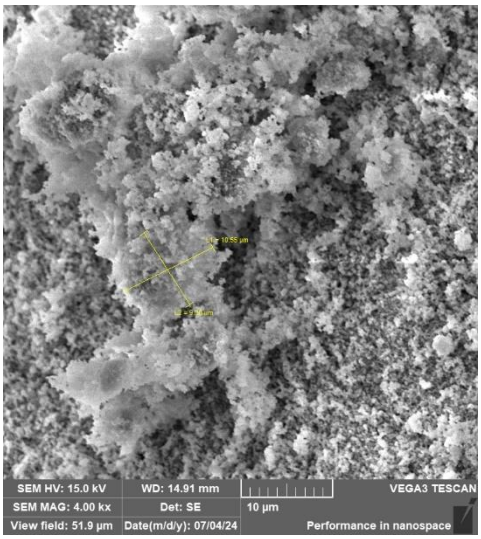

(e)

Figures 2. *SEM; (a) TiO2, (b) Fe-doped TiO2, (c) Zn-doped TiO2, (d) Mg-doped TiO2, dan (e) Cu-doped TiO2*

SEM analysis showed significant variations in particle morphology from TiO_2, Fe-doped TiO_2, Zn-doped TiO_2, Mg-doped TiO_2, and Mg-doped TiO_2 samples. The particle size for pure TiO_2 is relatively large (L1 = 31.01µm and L2 = 24.50 µm), which results in low specific surface area and hence reduced dye adsorption which potentially decreases the electron transfer efficiency in DSSC. In contrast, Fe-doped TiO_2 exhibits much smaller particle sizes (L1 = 13.96µm and L2 = 17.57 µm), increasing the specific surface area and allowing for greater adsorption of dyes as well as increased electron conductivity, thanks to Fe doping that can create useful electron centers.

Zn-doped TiO_2 has a very large particle size (L1 = 31.84µm and L2 = 39.53 µm), larger than pure TiO_2 which shows weakness in terms of specific surface area and dye application efficiency. This allows reducing the effectiveness of Zn-doped TiO_2 in DSSC. In contrast, Mg-doped TiO_2 exhibits smaller particle sizes (L1 = 18.32µm and L2 = 11.94 µm) which can increase the specific surface area and dye absorption capacity and can improve conductivity and electron transfer.

Cu-doped TiO_2 displays the smallest particle size (L1 = 10.55µm and L2 = 9.30 µm) showing a significant increase in specific surface area. Thus, Cu-doped TiO_2 has the highest performance potential in DSSC.

Table 2. *EDX Analysis Mapping Element Results Data*

Sample	Element	Content		
		Mass (%)	Mass Norm. (%)	Atom (%)
TiO_2	Ti	18.65	54.79	28.82
	O	15.39	45.21	71.18
Fe-doped TiO_2	Ti	17.69	50.13	25.23
	O	17.49	49.57	74.64
	Fe	0.11	0.30	0.13

	Ti	28.55	55.72	80.04
Zn-doped TiO_2	O	17.51	34.16	0.50
	Zn	5.19	10.12	0.16
	Ti	18.59	27.97	0.53
Mg-doped TiO_2	O	45.89	71.57	1.79
	Mg	0.45	0.46	0.03
	Ti	22.56	80.34	2.48
Cu-doped TiO_2	O	16.34	19.45	0.47
	Cu	0.23	0.21	0.03

Pure TiO_2 samples showed results in Ti and O proportions that could provide good basic stability but did not provide additional adsorption centers or significant conductivity improvements. Fe-doped TiO_2 has an additional Fe of 0.30% which can create an additional active center for electron transfer and increase the surface area for dye adsorption. However, the low concentration of Fe also means that the increase may be limited and should be optimized to get maximum results.

Zn-doped TiO_2 showed a significant increase in the mass of O (55.72%) with a small amount of Zn (10.12%) which allowed to improve structural stability and adsorption ability, the presence of high O could also indicate an excess oxidation that may not always be positive. Mg-doped TiO_2 with 0.46% Mg and 71.57 O shows a good balance in increasing dye adsorption and electron transfer, but the significant effect of Mg doping may affect the overall structure and may cause instability if the concentration is too high. Cu-doped TiO_2 with 2.48% Cu based on normative mass showed a very positive influence in improving DSSC performance. The presence of Cu significantly increases the active center for dye adsorption and electron transfer which can improve the overall efficiency of DSSC.

3.3. Chemical Characterization

Chemical characterization using Fourier Transform Infrared Spectroscopy (FTIR) analysis is used to identify various functional groups in a sample by showing the spectrum of infrared absorption intensity as a function of the wavelength or wave number. The FTIR spectrum can be seen in figure 3.

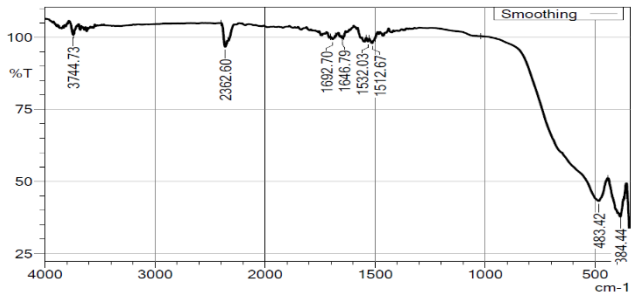

(a)

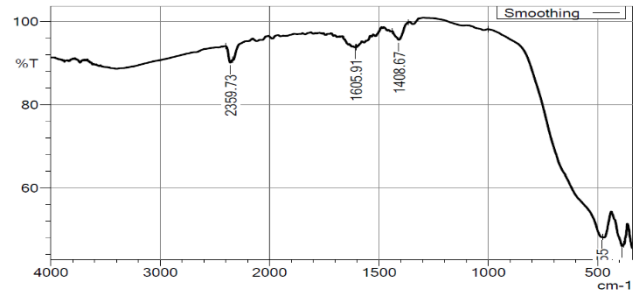

(b)

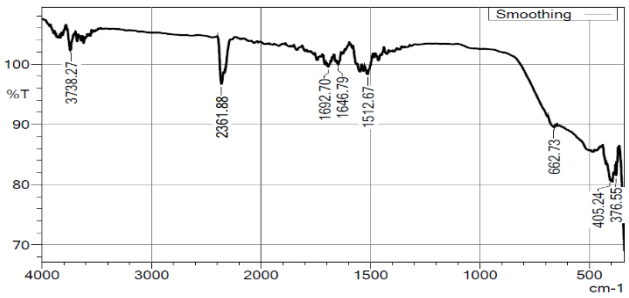

(c)

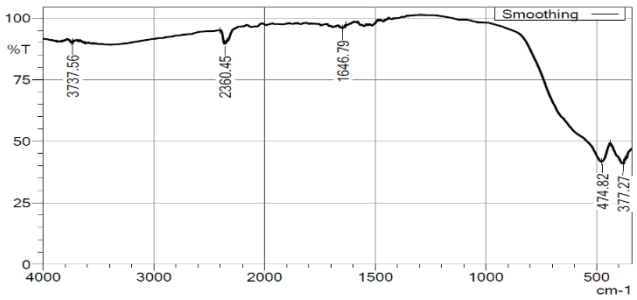

(d)

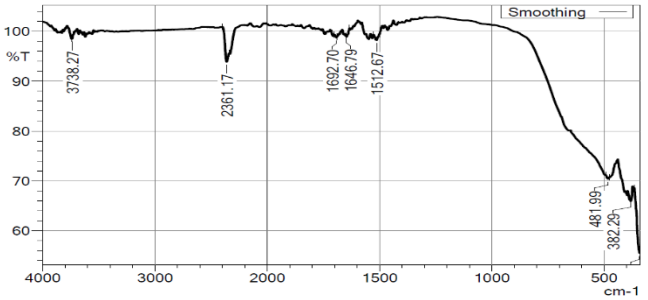

(e)

Figure 3. *Spectrum FTIR; (a) TiO_2, (b) Fe-doped TiO_2, (c) Zn-doped TiO_2, (d) Mg-doped TiO_2, dan (e) Cu-doped TiO_2*

The peak list data from the FTIR analysis can be seen in Table 3 - 7.

Table 3. *Peak List Data Results of FTIR analysis of TiO_2 sample*

No	Peak	Intensity	Base (H)	Base (L)	Area
1	384.44	37.78	385.16	371.53	813.299
2	483.42	43.17	1019.92	443.26	14825.469
3	1512.67	97.94	1526.29	1500.47	33.195
4	1532.03	98.53	1539.92	1526.29	12.479
5	1646.79	99.60	1648.94	1642.49	0.990
6	1692.70	99.29	1701.30	1680.50	3.866
7	2362.60	96.63	2399.18	2340.37	0.130
8	3744.73	100.82	3766.25	3743.30	-56.139

Table 4. *Peak List Data Results of FTIR analysis of Fe-doped TiO_2 sample*

No	Peak	Intensity	Base (H)	Base (L)	Area
1	387.31	46.03	388.03	380.86	386.285
2	480.55	48.17	1001.99	477.68	12346.30
3	1408.67	95.59	1438.79	1367.07	199.482
4	1605.91	93.74	1607.34	1602.32	31.223
5	2359.73	90.09	2399.90	2339.65	502.278

Table 5. *Data Peak List Hasil analisa FTIR sampel Zn-doped TiO2*

No	Peak	Intensity	Base (H)	Base (L)	Area
1	376.55	81.53	380.86	373.68	124.440
2	405.24	80.74	418.87	403.09	285.033
3	662.73	89.53	688.55	659.86	283.044
4	1512.67	98.31	1526.29	1500.47	26.214
5	1646.79	99.89	1648.94	1642.49	-0.641
6	1692.70	99.52	1701.30	1680.50	0.378
7	2361.88	96.69	2398.46	2340.37	9.787
8	3738.27	102.35	3739.71	3729.67	-29.814

Table 6. *Peak List Data Results of FTIR analysis of Zn-doped TiO_2 sample*

No	Peak	Intensity	Base (H)	Base (L)	Area
1	377.27	40.76	378.70	372.25	376.935
2	474.82	41.73	476.25	438.24	2091.457
3	1646.79	95.87	1648.94	1633.16	56.773
4	2360.45	89.53	2399.18	2339.65	488.253
5	3737.56	89.92	3738.99	3728.95	98.758

Table 7. *Peak List Data Results of FTIR analysis of Mg-doped TiO_2 sample*

No	Peak	Intensity	Base (H)	Base (L)	Area
1	342.13	55.51	364.36	339.97	956.378
2	382.29	65.93	385.16	380.86	145.627
3	481.99	70.40	492.75	476.97	462.561
4	1512.67	98.24	1526.29	1500.47	31.386
5	1646.79	98.91	1648.94	1633.88	6.888
6	1692.70	98.74	1701.30	1689.11	12.050
7	2361.17	93.89	2399.18	2340.37	193.509
8	3738.27	98.50	3739.71	3729.67	11.606

Based on the results of the analysis using FTIR, it was shown that the identification of the functional group contained functional groups such as hydroxyl (OH), adsorbed water, carbonyl (C=O), and possibly CO_2. In particular, the TiO_2 sample contained a Ti-O functional group, Fe-doped TiO_2 contained a Ti-O-Fe functional group, Zn-doped TiO_2 contained a Ti-O-Zn functional group, Mg-doped TiO_2 contained a Ti-O-Mg functional group, and Cu-doped TiO_2 contained a Ti-O-Cu functional group. The presence of hydroxyl groups and water can lead to degradation and decrease efficiency if not managed properly. The presence of carbonyl and CO_2 contaminants can also affect the performance and stability of DSSC.

Doping with metals such as Fe, Zn, Mg, and Cu results in shifts and changes in the intensity of the absorption peak that indicate modifications to the structure and surface of the material. Doping Fe adds a functional group that enriches the structure of TiO_2, increasing the absorption area significantly but with a less high intensity. Zn-doped TiO_2 exhibits high intensity but a less extensive area, suggesting surface modifications that may not be completely homogeneous.

Mg-doped TiO_2 has a strong surface modification with a large absorption area so that it can increase the adsorption capacity of dyes but also has low stability potential. Meanwhile, Cu-doped TiO_2 has a significant influence on structure and adsorption with a wide area, especially at lower wave numbers, indicating a strong interaction between Cu ions and TiO_2 matrices.

3.4. Optical Characterization

Light absorption measurements are performed in the UV light to visible light region (270-700 nm). The results of the UV-Vis analysis of telang flowers can be seen in Figure 4 and Table 7.

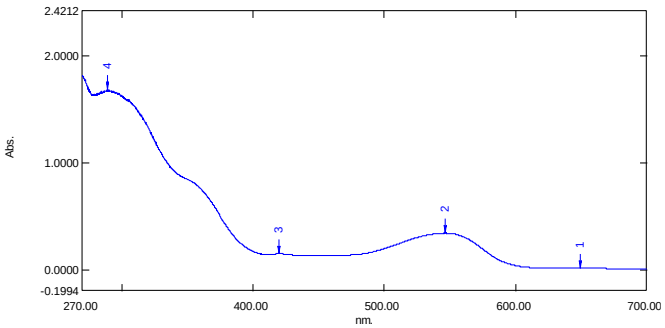

Figure 4. *Spectrum Peak Clitoria Ternatea*

Tabel 7. *Wavelenght and Absorbance of Absorbansi Clitoria Ternatea*

No	*Wavelenght*	*Absorbance*
1	649.30 nm	0.0172
2	546.30 nm	0.3417
3	419.80 nm	0.1475
4	289.00 nm	1.6858

At the wavelength of 649.30 nm, there is a low absorption of light (0.0172), suggesting that the anthocyanin molecule may undergo a less efficient energy transition at this wavelength. This can be caused by a number of factors, including changes in molecular conformation or possible interactions with solvents that affect the optic properties of the molecule.

The wavelength of 546.30 nm indicates high absorption and is likely the peak wavelength (λmax) at which anthocyanins absorb light with maximum intensity (0.3417). Significant electronic energy transitions or molecular conformations may occur at these wavelengths so that they are effective for producing electronic energy and contribute significantly to the efficiency of DSSC.

At a wavelength of 419.80 nm, there is moderate light absorption (0.1475). This may lie beyond peak wavelengths, and this moderate absorption capacity can be explained as the effect of a lower energy transition or molecular structural changes.

A very high absorption (1.6858) at a wavelength of 289 nm indicates the presence of a significant phenomenon. There may be a strong electronic energy transition or a drastic change in molecular conformation.

4. Conclusion

The results of characterization using XRD, SEM-EDX, FTIR analysis showed that doping on TiO_2 with Fe, Zn, Mg, and Cu provided a variety of variations. The results of XRD analysis revealed that doping modified the crystal structure of TiO_2 with Cu-doped TiO_2 showing the most significant changes. SEM-EDX indicates that element doping creates different morphologies that affect particle size and distribution where Cu-doped TiO_2 shows the most optimal morphology for electron transfer and dye absorption. FTIR confirms changes in functional groups and chemical bonds due to doping that affect the interaction of dye molecules and conductivity. Meanwhile, UV-Vis shows that Clitoria ternatea shows high absorbance at peak wavelengths which has the potential to have good light absorption efficiency, especially at optimal wavelengths.

Acknowledgements

The authors want to be acknowledged the Renewable Energy Engineering Department, Politeknik Negeri Sriwijaya, and PPM Dit. APTV through Contract No. 55/SPK/D.D4/PPK.01.APTV/III/2024 for funding supports this Master's Thesis Research. The Authors also thank Politeknik Negeri Sriwijaya for the supporting academic atmosphere.

References

[1] R. Ploetz, "Renewable Energy: Advantages and Disadvantages," Walsrode, 2016.

[2] V. Madurai Ramakrishnan *et al.*, "Performance of TiO2 nanoparticles synthesized by microwave and solvothermal methods as photoanode in dye-sensitized solar cells (DSSC)," *Int J Hydrogen Energy*, vol. 45, no. 51, pp. 27036–27046, Oct. 2020, doi: 10.1016/j.ijhydene.2020.07.018.

[3] A. Hayat, A. E. E. Putra, N. Amaliyah, and S. S. Pandey, "Clitoria ternatea flower as natural dyes for Dye-sensitized solar cells," in *IOP Conference Series: Materials Science and Engineering*, Institute of Physics Publishing, Oct. 2019. doi: 10.1088/1757-899X/619/1/012049.

[4] M. S. Ahmad, A. K. Pandey, N. A. Rahim, S. Shahabuddin, and S. K. Tyagi, "Chemical sintering of TiO2 based photoanode for efficient dye sensitized solar cells using Zn nanoparticles," *Ceram Int*, vol. 44, no. 15, pp. 18444–18449, Oct. 2018, doi: 10.1016/j.ceramint.2018.07.062.

[5] F. A. Unal, S. Ok, M. Unal, S. Topal, K. Cellat, and F. Şen, "Synthesis, characterization, and application of transition metals (Ni, Zr, and Fe) doped TiO2 photoelectrodes for dye-sensitized solar cells," *J Mol Liq*, vol. 299, Feb. 2020, doi: 10.1016/j.molliq.2019.112177.

[6] R. Musiana, A. Hasan, and R. D. Kusumanto, "Titanium Dioxide Soaking Time Effects on DSSC Powers and Efficiency," 2021.

[7] Y. Nadhirah, R. Kusumanto, and A. Hasan, "Increasing Efficiency of Dye-Sensitized Solar Cell (DSSC) Originating from Yellow Sweet Potato Extract as Dye Sensitizer: Effect of Acetic Acid, Polyethylene Glycol, and Polyvinyl Alcohol as TiO2 binders," *Jurnal Kimia Sains dan Aplikasi*, vol. 23, no. 11, pp. 403–408, Nov. 2020, doi: 10.14710/jksa.23.11.403-408.

[8] R. S. Dubey, K. V. Krishnamurthy, and S. Singh, "Experimental studies of TiO2 nanoparticles synthesized by sol-gel and solvothermal routes for DSSCs application," *Results Phys*, vol. 14, Sep. 2019, doi: 10.1016/j.rinp.2019.102390.

[9] K. Athira, K. T. Merin, T. Raguram, and K. S. Rajni, "Synthesis and characterization of Mg doped TiO2 nanoparticles for photocatalytic applications," *Mater Today Proc*, vol. 33, pp. 2321–2327, 2020, doi: 10.1016/j.matpr.2020.04.580.

[10] S. Mehraz, P. Kongsong, A. Taleb, N. Dokhane, and L. Sikong, "Large scale and facile synthesis of Sn doped TiO2 aggregates using hydrothermal synthesis," *Solar Energy Materials and Solar Cells*, vol. 189, pp. 254–262, Jan. 2019, doi: 10.1016/j.solmat.2017.06.048.

[11] M. Shakeel Ahmad, A. K. Pandey, and N. A. Rahim, "Towards the plasmonic effect of Zn nanoparticles on TiO2 monolayer photoanode for dye sensitized solar cell applications," *Mater Lett*, vol. 195, pp. 62–65, May 2017, doi: 10.1016/j.matlet.2017.02.099.

[12] X. J. Yang, S. Wang, H. M. Sun, X. B. Wang, and J. S. Lian, "Preparation and photocatalytic performance of Cu-doped TiO2 nanoparticles," *Transactions of Nonferrous Metals Society of China (English Edition)*, vol. 25, no. 2, pp. 504–509, Feb. 2015, doi: 10.1016/S1003-6326(15)63631-7.

[13] J. Wang *et al.*, "The effects of additive on properties of Fe doped TiO2 nanoparticles by modified sol-gel method," *J Alloys Compd*, vol. 858, Mar. 2021, doi: 10.1016/j.jallcom.2020.157726.

[14] N. Rathore, R. K. Shukla, K. C. Dubey, and A. Kulshreshtha, "Synthesis of undoped and Fe doped nanoparticles of TiO2via co-precipitation technique and their characterizations," in *Materials Today: Proceedings*, Elsevier Ltd, 2019, pp. 861–865. doi: 10.1016/j.matpr.2020.05.072.

[15] N. Kanjana, W. Maiaugree, P. Poolcharuansin, and P. Laokul, "Synthesis and characterization of Fe-doped TiO2 hollow spheres for dye-sensitized solar cell applications," *Mater Sci Eng B Solid State Mater Adv Technol*, vol. 271, Sep. 2021, doi: 10.1016/j.mseb.2021.115311.

[16] S. M. Amir-Al Zumahi *et al.*, "Understanding the optical behaviours and the power conversion efficiency of novel organic dye and nanostructured TiO2 based integrated DSSCs," *Solar Energy*, vol. 225, pp. 129–147, Sep. 2021, doi: 10.1016/j.solener.2021.07.024.

[17] M. Yahya, A. Bouziani, C. Ocak, Z. Seferoğlu, and M. Sillanpää, "Organic/metal-organic photosensitizers for dye-sensitized solar cells (DSSC): Recent developments, new trends, and future perceptions," *Dyes and Pigments*, vol. 192. Elsevier Ltd, Aug. 01, 2021. doi: 10.1016/j.dyepig.2021.109227.

[18] I. Izirwan, T. D. Munusamy, N. H. Hamidi, and S. Z. Sulaiman, "Optimization of microwave-assisted extraction of anthocyanin from clitoria ternatea flowers," *International Journal of Mechanical Engineering and Robotics Research*, vol. 9, no. 9, pp. 1246–1252, Sep. 2020, doi: 10.18178/ijmerr.9.9.1246-1252.

[19] S. Shalini, R. Balasundara Prabhu, S. Prasanna, T. K. Mallick, and S. Senthilarasu, "Review on natural dye sensitized solar cells: Operation, materials and methods," *Renewable and Sustainable Energy Reviews*, vol. 51. Elsevier Ltd, pp. 1306–1325, Aug. 01, 2015. doi: 10.1016/j.rser.2015.07.052.

[20] N. A. Karim, U. Mehmood, H. F. Zahid, and T. Asif, "Nanostructured photoanode and counter electrode materials for efficient Dye-Sensitized Solar Cells (DSSCs)," *Solar Energy*, vol. 185. Elsevier Ltd, pp. 165–188, Jun. 01, 2019. doi: 10.1016/j.solener.2019.04.057.

[21] L. Zhou *et al.*, "Improved performance of dye sensitized solar cells using Cu-doped TiO2 as photoanode materials: Band edge movement study by spectroelectrochemistry," *Chem Phys*, vol. 475, pp. 1–8, Aug. 2016, doi: 10.1016/j.chemphys.2016.05.018.

[22] J. E. Ikpesu, S. E. Iyuke, M. Daramola, and A. O. Okewale, "Synthesis of improved dye-sensitized solar cell for renewable energy power generation," *Solar Energy*, vol. 206. Elsevier Ltd, pp. 918–934, Aug. 01, 2020. doi: 10.1016/j.solener.2020.05.002.